文章编号: 1001-9014(2019)05-0549-05 DOI: 10.11972/j.issn.1001-9014.2019.05.001

Wet etching for InAs-based InAs/Ga(As)Sb superlattice long wavelength infrared detectors

WU Jia[1,2], XU Zhi-Cheng[1], CHEN Jian-Xin[1*], HE Li[1]

(1. Key Laboratory of Infrared Imaging Materials and Detector, Shanghai Institute of Technical Physics, Chinese Academy of Sciences, Shanghai 200083, China;
2. University of Chinese Academy of Sciences, Beijing 100049, China)

Abstract: Wet chemical etching of InAs-based InAs/Ga(As)Sb superlattice long wavelength infrared photodiodes was studied in this paper. The etching experiments using citric acid, orthophosphoric acid and hydrogen peroxide were carried out on InAs, GaSb bulk materials and InAs/Ga(As)Sb superlattices with different solution ratios. An optimized etching solution for the InAs-based superlattices has been obtained. The etched surface roughness is only 1 nm. InAs-based superlattice LWIR detectors with 50 % cut-off wavelength of 12 μm were fabricated. The photodetectors etched with optimized solution ratio show low surface leakage characteristic. At 81 K temperature, the surface resistivity $\rho_{Surface}$ of the detector is 4.4×10^3 Ωcm.

Key words: InAs/Ga(As)Sb, type-II superlattice, wet chemical etching, surface morphology
PACS: 81.05.Ea

InAs基InAs/Ga(As)Sb II类超晶格长波红外探测器湿法腐蚀研究

吴 佳[1,2], 徐志成[1], 陈建新[1*], 何 力[1]

(1. 中国科学院上海技术物理研究所 红外成像材料与器件重点实验室,上海 200083;
2. 中国科学院大学,北京 100049)

摘要:开展了InAs基InAs/Ga(As)Sb II类超晶格长波红外探测器的湿法腐蚀工艺研究.选择的腐蚀液由柠檬酸、磷酸和过氧化氢组成,先后在InAs、GaSb体材料和InAs/Ga(As)Sb II类超晶格上进行了湿法腐蚀实验,分别获得了其最佳的腐蚀液组分及配比.使用优化的磷酸系腐蚀液对InAs/Ga(As)Sb II类超晶格进行腐蚀,获得的腐蚀表面粗糙度仅为1 nm.然后使用改进的工艺制备了50 %截止波长为12 μm的超晶格长波单元器件,实验结果表明磷酸系腐蚀液可以获得低暗电流密度的InAs基InAs/Ga(As)Sb II类超晶格长波红外探测器.另外,在81 K下,该探测器的表面电阻率($\rho_{Surface}$)为4.4×10^3 Ωcm.

关 键 词:InAs/Ga(As)Sb;II类超晶格;湿法腐蚀;表面形貌
中图分类号:TN213 **文献标识码**:A

Introduction

Long wavelength infrared (LWIR) photo-detectors have important applications in the fields of geoexploration, marine and environmental monitoring, meteorological forecast, etc. InAs/GaSb Type-II superlattices (SLs) have showed excellent opto-electrical properties for infrared detection and high performance focal plane arrays based on this novel material have been demonstrated [1-3,20-22]. Up to now, InAs/GaSb superlattice materials are mainly grown on GaSb substrates. There exists strain in the GaSb-based InAs/GaSb superlattice since the lat-

Received date: 2019-01-12, **revised date**: 2019-07-08 **收稿日期**:2019-01-12,**修回日期**:2019-07-08
Foundation items: Supported by the National Natural Science Foundation of China (61534006, 61974152, 61505237, 61505235, 61404148, 61176082), the National Key Research and Development Program of China (2016YFB0402403), and the Youth Innovation Promotion Association, CAS (2016219)
Biography: WU Jia (1991-), male, Hangzhou, Zhejiang, Ph. D. Research fields focus on properties of antimonide superlattice materials and photodetectors. E-mail: wujia_0128@163.com
[*] **Corresponding author**: E-mail: jianxinchen@mail.sitp.ac.cn

tice constant of InAs is smaller than that of GaSb. Though the strain, in one hand, can enhance the opto-electrical properties of the superlattice, such as helping to split off the heavy and light hole bands, in the other hand, it put challenges on epitaxial growth. The challenge turns bigger when the cutoff wavelength of the SLs extends to long wavelength regions since the InAs layers in the superlattice are getting thicker [4-5]. Therefore, the lattice matched InAs/Ga(As)Sb superlattices on InAs substrates as an alternative to the conventional GaSb-based InAs/GaSb superlattices for LWIR photodetectors was proposed by our laboratory. Then, the high material quality and promising optical-electrical properties of the InAs-based InAs/Ga(As)Sb superlattices was demonstrated by our laboratory [6-8]. Due to the ability to pattern semiconductors in an anisotropic and uniform way, dry etching is suitable for small-size mesa preparation, while wet etching is simple, fast, and no crystallographic damage to the etched surface, which is suitable for large-size mesa preparation [9-10,19]. Therefore, the wet chemical etching was studied for this novel superlattice in this paper.

Numerous wet chemical etchants have been investigated on GaSb-based InAs/GaSb type-II superlattice materials [11-14]. Best results were obtained by using citric acid ($C_6H_8O_7$), orthophosphoric acid (H_3PO_4) and hydrogen peroxide (H_2O_2) with an appropriate solution ratio [15]. An optimized solution ratio for GaSb-based SL etching cannot be directly applied to InAs-based SL materials since the InAs and GaSb binaries present very different physical - chemistry properties and the etching process for the two compounds are very different [16]. Moreover, slight changes in etchant component ratios can result in large changes in etch rate and mesa sidewall roughness of the superlattice materials [17]. Therefore, the InAs-based SL wet etching process has to be studied systematically to achieve high performance photodetectors.

1 Experiment

Wet chemical etching experiments were first carried out on InAs and GaSb bulk materials, all samples were processed into mesas using standard optical lithography and wet chemical etching with the chemical solution based on citric acid ($C_6H_8O_7$, 100 %), orthophosphoric acid (H_3PO_4, 85 %) and hydrogen peroxide (H_2O_2, 30 %). The wet etching rate and roughness of mesa sidewalls were measured by step profiler and atomic force microscope (AFM), respectively. Then the optimized etching solution was applied to fabricate single pixel InAs-based SL detectors. The InAs-based superlattices were grown by molecular beam epitaxy. The layered structure of the InAs-based T2SLs long wavelength infrared detector was shown in Figure 1, consisted of a 1 μm Si-doped InAs buffer layer, followed by a 50 period Si-doped 22 ML InAs/9 ML Ga(As)Sb n-type superlattice, a 200 period lightly Be-doped 22 ML InAs/9 ML Ga(As)Sb absorber region, a 50 period Be-doped 22 ML InAs/9 ML Ga(As)Sb p-type superlattice, and finally a 50 nm Be-doped GaSb cap layer. The detectors are designed to receive the irradiance from the front sides. The architecture of the single-pixel detectors can be found in our previous paper.

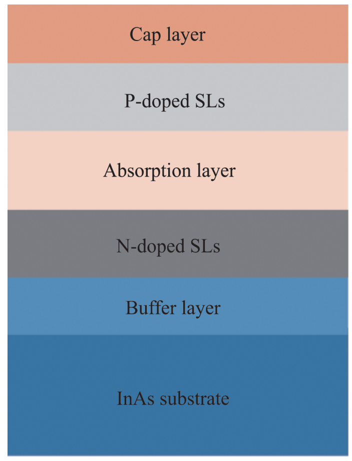

Fig. 1 The layered structure of the InAs-based T2SLs long wavelength infrared detector.

图1 InAs基II类超晶格长波探测器的分层结构

2 Result and discussion

2.1 Etching of InAs and GaSb bulk materials

The chemical reactions of InAs and GaSb etching with citric acid ($C_6H_8O_7$), orthophosphoric acid (H_3PO_4) and hydrogen peroxide (H_2O_2) are as follows,

$$2GaSb + 6H_2O_2 \rightarrow Ga_2O_3 + Sb_2O_3 + 6H_2O \quad . \quad (1)$$

$$2InAs + 6H_2O_2 \rightarrow In_2O_3 + As_2O_3 + 6H_2O \quad . \quad (2)$$

$$InAs + 4H_2O_2 \rightarrow InAsO_4 + 4H_2O \quad . \quad (3)$$

$$2M_2O_3 + 7H_3PO_4 \rightarrow M(H_2PO_4)_3 + M_2(HPO_4)_3 + MPO_4 + 6H_2O \quad . \quad (4)$$

(M = Ga or As or Sb or In)

$$Sb_2O_3 + 2C_6H_8O_7 \rightarrow 2(Sb(C_6H_4O_7)(H_2O)) + H_2O + 2H^+ \quad . \quad (5)$$

Among the above chemical reactions, H_2O_2 is the oxidizing agent. InAs and GaSb oxidized with H_2O_2 firstly, then the products are dissolved in water or reacted with H_3PO_4. Sb_2O_3 is poorly soluble in water or H_3PO_4, while it can react with $C_6H_8O_7$ to form a water-soluble complex. Therefore etchants containing $C_6H_8O_7$ is necessary for GaSb, while etchants without $C_6H_8O_7$ is feasible for InAs.

The etching rate and surface roughness with different etchants for InAs bulk materials were shown in Table 1. When $H_3PO_4:H_2O_2 = 1:1$ and without $C_6H_8O_7$, the surface is the smoothest and the roughness is only 0.4 nm, which was shown in Figure 2(a). While maintaining the ratio of $H_3PO_4:H_2O_2 = 1:1$, the surface roughness is increased with increasing the proportion of $C_6H_8O_7$. The presence of $C_6H_8O_7$ does not improve the InAs mesa sidewalls morphology, similar to reports in the literature [18]. When the proportion of H_2O_2 is slightly more than that of H_3PO_4, it has little effect on the surface roughness, while the surface roughness is increased with increasing H_3PO_4 content. That is because if H_3PO_4 content is increased, the dihydrogen phosphate will further react with H_3PO_4, which lead to form a poorly soluble salt (monohydrogen

Table 1　Etching rate and surface roughness with different etchants for InAs bulk materials.

表 1　InAs体材料表面腐蚀速率和粗糙度随腐蚀液组分和配比的变化

$C_6H_8O_7:H_3PO_4:H_2O_2$	Etching rate (μm/min)	Surface roughness (nm)
0:0.1:1	0.26	1.4
0:0.5:1	0.35	0.5
0:1:1	0.45	0.4
0:5:1	0.35	10.9
0:10:1	0.25	15.6
0.2:1:1	0.33	1.1
1:1:1	0.32	2.7

phosphate or normal phosphate). The presence of these complexes will adsorb on the mesa sidewalls to form a dense film and prevent the etching reaction to continue and strongly deteriorate the mesa surface sidewalls morphology[15].

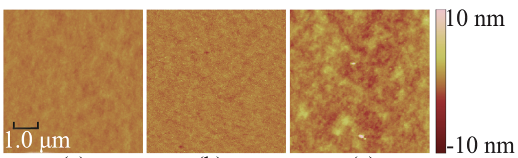

Fig. 2　AFM pictures of the etching surface of (a) InAs bulk material, (b) GaSb bulk material and (c) InAs-based superlattices with the optimized etchants, respectively.

图 2. (a)InAs体材料(b)GaSb体材料和(c)InAs基超晶格材料分别在使用优化的腐蚀工艺后，测得的腐蚀表面的AFM形貌图

The etching rate and surface roughness with different etchants for GaSb bulk materials were shown in Table 2. For the wet etching of GaSb, $C_6H_8O_7$ have to be contained as a complexing agent to react with Sb_2O_3 to form a soluble product. When $C_6H_8O_7$: H_3PO_4: H_2O_2 = 10:1:1, the smoothest surface was obtained and the roughness is only 0.7 nm, which was shown in Figure 2 (b). The surface roughness is gradually increased with reducing the proportion of $C_6H_8O_7$. And the surface roughness is gradually increased with increasing the proportion of H_3PO_4, while when the proportion of H_2O_2 is more than that of H_3PO_4, the surface roughness change slightly. This is similar to the results of InAs bulk materials.

2.2　Etching of InAs-based superlattices

Through the above experiments, it was found that for InAs-based SL materials, H_2O_2 was used as an oxidant, H_3PO_4 was used to react with the oxide products and $C_6H_8O_7$ was used as a complexing agent. The optimized proportion of H_2O_2 and H_3PO_4 is around 1:1 and the proportion of H_2O_2 can be slightly more than that of H_3PO_4. The $C_6H_8O_7$ content in the etching etchants is related to the Ga(As)Sb thickness ratio in InAs-based superlattice.

Table 2　Etching rate and surface roughness with different etchants for GaSb bulk materials.

表 2　GaSb体材料表面腐蚀速率和粗糙度随腐蚀液组分和配比的变化

$C_6H_8O_7:H_3PO_4:H_2O_2$	Etching rate (μm/min)	Surface roughness (nm)
10:1:1	0.32	0.7
3:1:1	0.45	1.5
1:1:1	0.86	2.4
10:1.5:1	1.2	6.8
10:1:3	0.26	1.1

Keeping H_2O_2: H_3PO_4 = 1: 1 and adding $C_6H_8O_7$, the etching rate and surface roughness with different etchants for InAs-based superlattices were investigated, as shown in Table 3. When $C_6H_8O_7$: H_3PO_4: H_2O_2 = 3:1:1, the surface roughness is the smallest, only 1 nm. The AFM picture was shown in Figure 2 (c).

Table 3　Etching rate and surface roughness with different etchants for InAs-based superlattices

表 3　InAs基超晶格材料表面腐蚀速率和粗糙度随腐蚀液组分和配比的变化

$C_6H_8O_7:H_3PO_4:H_2O_2$	Etching rate (μm/min)	Surface roughness (nm)
10:1:1	0.32	8.3
3:1:1	0.45	1.0
1:1:1	1.2	3.5

The InAs-based superlattice LWIR detector was fabricated by the optimized etchants of $C_6H_8O_7$: H_3PO_4: H_2O_2 = 3:1:1 (Sample 311). At the same time, another sample was used for comparison that etched by the etchants of $C_6H_8O_7$: H_3PO_4: H_2O_2 = 10: 1: 1 (Sample 1011). The SEM pictures of the InAs-based superlattice mesa sidewalls of (a) sample 1011 and (b) sample 311 were shown in Fig. 3. The etching surface of sample 311 is smoother than that of sample 1011.

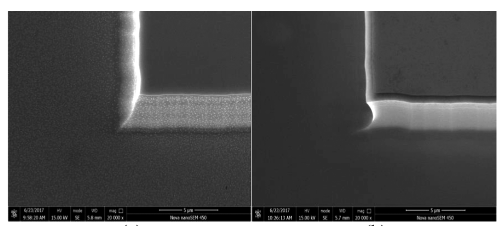

Fig. 3　SEM pictures of the InAs-based SL photodetectors etched with (a) $C_6H_8O_7$:H_3PO_4:H_2O_2 = 10:1:1 and (b) $C_6H_8O_7$:H_3PO_4:H_2O_2 = 3:1:1 at room temperature.

图 3　在室温下，分别使用腐蚀液(a)$C_6H_8O_7$:H_3PO_4:H_2O_2 = 10:1:1 和(b)$C_6H_8O_7$:H_3PO_4:H_2O_2 = 3:1:1 制备InAs基超晶格单元器件时，获得的器件腐蚀表面和侧壁的SEM图

Figure 4 (a) shows the current responsivity spectrum of the InAs-based SL detector measured at 81 K. The 50 % cut-off wavelength of the detectors reaches 12 μm. The fabricated photodiodes have a similar peak responsivity of 1.6 A/W at 81 K, corresponding to quantum efficiency (QE) of 38 %. Figure 4 (b) shows the dark current density and dynamic differential resistance-area product values (RA) of sample 311 (red dots) and sample 1011 (black dots) with mesa area of 200 × 200 μm^2. The dark current density of sample 311 and sample 1011 are 5.7×10^{-3} A/cm^2 and 9.2×10^{-3} A/cm^2, respectively, under a bias of -20 mV at 81 K. The surface resistivity $\rho_{Surface}$ of two samples were calculated by a linear least squares fitting (see Figure 4 c) between the R_0A^{-1} (R_0A denotes the differential-resistance-area-product at zero bias) of diodes and P/A ratio based on the following equation:

$$\frac{1}{R_0A} = \frac{1}{R_0A_{Bulk}} + \frac{1}{\rho_{Surface}}\frac{P}{A} \quad , \quad (6)$$

Where R_0A_{bulk} is the bulk differential-resistance-area-product, P is the perimeter of the diode mesa, and A is the cross-sectional area of the detector. $\rho_{Surface}$ of sample 311 is 4.4×10^3 Ωcm, which is almost eight times larger than that (5.1×10^2 Ωcm) of sample 1011, indicating a good surface quality obtained by the optimized etchants and an InAs-based SL LWIR detector with enough low surface leakage currents has been fabricated.

3 Conclusion

Wet chemical etching of InAs-based InAs/Ga(As)Sb superlattice long wavelength infrared photodiodes was studied in this paper. The etching experiments using citric acid, orthophosphoric acid and hydrogen peroxide were carried out on InAs, GaSb bulk materials and InAs-based superlattices with different solution ratios. H_2O_2 was used as an oxidant, H_3PO_4 was used to react with the oxide products and $C_6H_8O_7$ was used as a complexing agent. The optimized proportion of H_2O_2 and H_3PO_4 is around 1:1 and the proportion of H_2O_2 can be slightly more than that of H_3PO_4. The $C_6H_8O_7$ content in the etching etchants is related to the Ga(As)Sb thickness ratio in InAs-based superlattice. An optimized etching solution for the InAs-based superlattices has been obtained. The etched surface roughness is only 1 nm. The InAs-based LWIR detectors with 50 % cut-off wavelength of 12 μm were fabricated. The photodetectors etched with optimized solution ratio show low surface leakage characteristic. At 81 K, the surface resistivity $\rho_{Surface}$ of the detector is 4.4×10^3 Ωcm.

Acknowledgment

This work was supported by the National Natural Science Foundation of China (NSFC) with Grant No. 61534006, 61505237, 61505235, 61404148, the National Key Research and Development Program of China with Grant No. 2016YFB0402403 and the Natural Science Foundation of Shanghai with Grant No. 15ZR1445600 and No. 16ZR1447900.

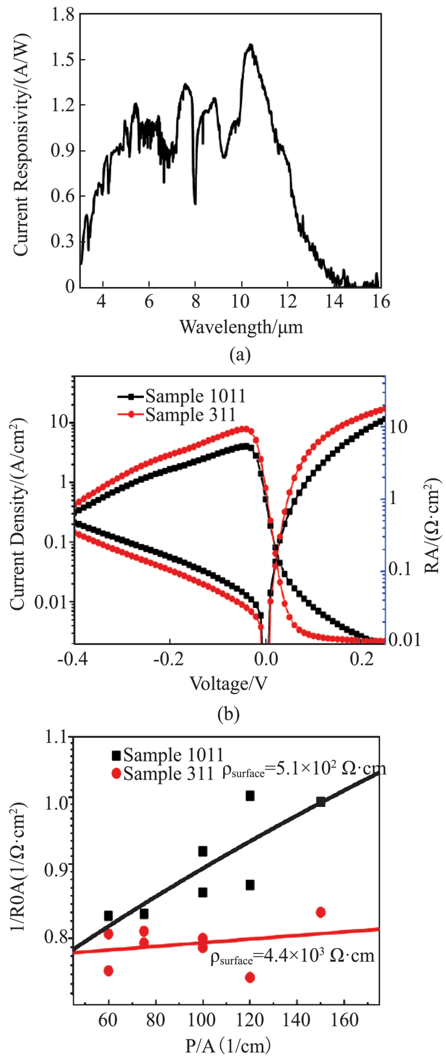

Fig. 4 (a) Current responsivity spectrum of detectors etched with $C_6H_8O_7$:H_3PO_4:H_2O_2 = 3:1:1 at 81 K (b) I-V characteristic for devices etched with $C_6H_8O_7$:H_3PO_4:H_2O_2 = 10:1:1 (black dots) and $C_6H_8O_7$:H_3PO_4:H_2O_2 = 3:1:1 (red dots) (c) The dependence of R_0A^{-1} at zero bias on P/A ratio for the two detectors at 81 K.

图4 (a)腐蚀液为$C_6H_8O_7$:H_3PO_4:H_2O_2 = 3:1:1时，在81 K下测得的器件的电流响应光谱；(b)在81 K下，腐蚀液分别为$C_6H_8O_7$:H_3PO_4:H_2O_2 = 10:1:1(黑点)和$C_6H_8O_7$:H_3PO_4:H_2O_2 = 3:1:1(红点)时，测得的暗电流密度和动态差分电阻面积乘积值(RA)随偏压的变化；(c)在81 K下，两个样品的R_0A^{-1}和P/A比之间的线性关系

References

[1] Kim H S, Plis E, Rodriguez J B, *et al*. Mid-IR focal plane array based on type-II InAs/GaSb strain layer superlattice detector with nBn design [J]. *Applied Physics Letters*, 2008, **92**(18): 183502.

[2] Manurkar P, Ramezani-Darvish S, Nguyen B M, *et al*. High performance long wavelength infrared mega-pixel focal plane array based on type-II superlattices [J]. *Applied Physics Letters*, 2010, **97**(19): 193505.

[3] Haddadi A, Ramezani-Darvish S, Chen G, *et al*. High operability 1024 × 1024 long wavelength Type-II superlattice focal plane array

[J]. *IEEE Journal of Quantum Electronics*, 2012, **48**(2): 221-228.

[4] Chen Y, Moy A, Mi K, *et al*. A highly strained InAs/GaSb type II superlattice for LWIR detection [C]//Nanophotonics and Macrophotonics for Space Environments VII. International Society for Optics and Photonics, 2013, **8876**: 887610.

[5] Walther M, Rehm R, Schmitz J, *et al*. InAs/GaSb type II superlattices for advanced 2nd and 3rd generation detectors [C]//Quantum Sensing and Nanophotonic Devices VII. International Society for Optics and Photonics, 2010, **7608**: 76081Z.

[6] Wang F, Chen J, Xu Z, *et al*. InAs-based InAs/GaAsSb type-II superlattices: Growth and characterization [J]. *Journal of Crystal Growth*, 2015, **416**: 130-133.

[7] Xu Z, Chen J, Wang F, *et al*. High performance InAs/GaAsSb superlattice long wavelength infrared photo-detectors grown on InAs substrates [J]. *Semiconductor Science and Technology*, 2017, **32**(5): 055011.

[8] Wang F, Chen J, Xu Z, *et al*. Performance comparison between the InAs-based and GaSb-based type-II superlattice photodiodes for long wavelength infrared detection [J]. *Optics express*, 2017, **25**(3): 1629-1635.

[9] Tan S L, Goh Y L, dip Das S, *et al*. Dry etching and surface passivation techniques for type-II InAs/GaSb superlattice infrared detectors [C]//Optics and Photonics for Counterterrorism and Crime Fighting VI and Optical Materials in Defence Systems Technology VII. International Society for Optics and Photonics, 2010, **7838**: 783814.

[10] Huang E K, Hoffman D, Nguyen B M, *et al*. Surface leakage reduction in narrow band gap type-II antimonide-based superlattice photodiodes [J]. *Applied Physics Letters*, 2009, **94**(5): 053506.

[11] Dier O, Lin C, Grau M, *et al*. Selective and non-selective wet-chemical etchants for GaSb-based materials [J]. *Semiconductor Science and Technology*, 2004, **19**(11): 1250.

[12] Mairiaux E, Desplanque L, Wallart X, *et al*. Selective wet chemical etching of GaInSb and AlInSb for 6.25 Å HBT fabrication [C]//Indium phosphide and related materials, 2008. IPRM 2008. 20th International Conference on. IEEE, 2008: 1-3.

[13] Kutty M N, Plis E, Khoshakhlagh A, *et al*. Study of surface treatments on InAs/GaSb superlattice LWIR detectors [J]. *Journal of Electronic Materials*, 2010, **39**(10): 2203-2209.

[14] Berishev I E, De Anda F, Mishournyi V A, *et al*. H_2O_2:HF:$C_4H_6O_6$ (tartaric acid):H_2O etching System for Chemical Polishing of GaSb [J]. *Journal of the Electrochemical Society*, 1995, **142**(10): L189-L191.

[15] Chaghi R, Cervera C, Aït-Kaci H, *et al*. Wet etching and chemical polishing of InAs/GaSb superlattice photodiodes [J]. *Semiconductor Science and Technology*, 2009, **24**(6): 065010.

[16] Song L, Degroote S, Choi K H, *et al*. Release of epitaxial layers grown on InAs substrates [J]. *Electrochemical and Solid-state Letters*, 2003, **6**(2): G25-G26.

[17] DeSalvo G C, Kaspi R, Bozada C A. Citric acid etching of $GaAs_{1-x}Sb_x$, $Al_{0.5}Ga_{0.5}Sb$, and InAs for heterostructure device fabrication [J]. *Journal of the Electrochemical Society*, 1994, **141**(12): 3526-3531.

[18] Marshall A R J, Tan C H, David J P R, *et al*. Fabrication of InAs photodiodes with reduced surface leakage current [C]//Optical Materials in Defence Systems Technology IV. International society for optics and photonics, 2007, **6740**: 67400H.

[19] Huang M, Chen J, Xu J, *et al*. ICP etching for InAs-based InAs/GaAsSb superlattice long wavelength infrared detectors [J]. *Infrared Physics & Technology*, 2018, **90**: 110-114.

[20] Klipstein P C, Avnon E, Benny Y, *et al*. Long wave infrared type II superlattice focal plane array detector [J]. *Defence Science Journal*, 2017, **67**(2): 135-140.

[21] Höglund L, Rodriguez J B, von Würtemberg R M, *et al*. Influence of shallow versus deep etching on dark current and quantum efficiency in InAs/GaSb superlattice photodetectors and focal plane arrays for long wavelength infrared detection [J]. *Infrared Physics & Technology*, 2018, **95**: 158-163.

[22] Chevallier R, Haddadi A, Razeghi M. Toward realization of small-size dual-band long-wavelength infrared photodetectors based on InAs/GaSb/AlSb type-II superlattices [J]. *Solid-State Electronics*, 2017, **136**: 51-54.